Uncertainty-Aware Carbon Flux Estimation from Multispectral Landsat Imagery Using Mixture Density Networks

Anish Dulal
Department of Computer Science
University of Oregon
anishd@uoregon.edu

Jake Searcy
Department of Data Science
University of Oregon
jsearcy@uoregon.edu

Abstract

Accurately quantifying carbon fluxes across ecosystems is essential for monitoring and validating natural climate solutions (NCS) which promise to mitigate climate change. Measurement methods, such as eddy covariance towers, provide ground truth data at high temporal resolution but suffer from limited spatial coverage. Upscaling these measurements to ecosystem scales is performed with machine learning methods based on environmental drivers and satellite data. However, correctly quantifying uncertainty in these predictions remains a challenge, which limits its use in carbon markets. We propose an uncertainty-aware carbon flux estimation framework that integrates multispectral Landsat imagery, EC flux measurements, and ancillary environmental variables using Mixture Density Networks. Our framework provides estimates of both aleatoric and epistemic uncertainties that enhance the reliability and scalability of carbon monitoring efforts.

1 Introduction

Natural Climate Solutions (NCS)—which involve the conservation, restoration, and improved management of natural ecosystems to enhance carbon sequestration—have emerged as important components of climate change mitigation strategies (Griscom et al., 2017; Seddon et al., 2020; Goldstein et al., 2020). A precise understanding of ecosystem carbon dynamics is crucial for informing climate models, guiding policy decisions, and upholding the integrity of carbon markets, particularly those incentivizing carbon sequestration through mechanisms such as carbon credits (Jacobson et al., 2018; CIB, 2021; Friedlingstein et al., 2023; Grassi et al., 2022; Baldocchi et al., 2003). Traditional methods, such as eddy covariance (EC) towers that provide continuous measurements of carbon dioxide exchange (Baldocchi et al., 2014), face challenges in scalability due to limited spatial coverage resulting from high costs and logistical hurdles (Pastorello et al., 2020). Moreover, while field campaigns measuring vegetation properties (e.g., tree height, diameter, and biomass) yield valuable ground-truth data (Asner et al., 2013), they are labor-intensive and impractical for large-scale application—a challenge underscored by the American Carbon Registry (ACR) (ACR, 2021). Remote sensing technologies offer a promising avenue for extrapolating point-based observations to broader scales (Turner et al., 2007), although translating high-dimensional satellite data into precise carbon flux estimates remains challenging due to ecological complexity and inherent observational uncertainties (ACR, 2020; Beer et al., 2010; Paoletti et al., 2019).

Recent studies have increasingly turned to machine learning techniques to address these challenges(Turner et al., 2007). However, they often yield point estimates that may not capture the full predictive distribution in either single or multimodal scenarios (Dietterich, 2000), and their reliance on manually engineered features can limit their ability to model complex non-linear relationships compared to deep learning approaches (Goodfellow et al., 2016). Neural networks have similarly been employed for carbon flux estimation yet their traditional designs typically produce deterministic outputs without inherent uncertainty quantification (Abdar et al., 2021). MDNs present an alternative by combining neural networks with probabilistic modeling to output parameters of a mixture of probability distributions rather than a single point estimate (Bishop, 1994). This approach captures both aleatoric and epistemic uncertainties and models complex, multimodal output distributions (Choi et al., 2021; Arnez et al., 2020), thereby delivering richer information than point estimates or simple uncertainty bounds while obviating the need for manual feature engineering. MDNs have demonstrated effectiveness across domains such as hydrology (Saranathan et al., 2024), meteorology (Kirkwood et al., 2022), and renewable energy forecasting (Men et al., 2016), underscoring their potential to provide reliable and scalable carbon flux estimates that are essential for evaluating progress toward climate goals and ensuring transparency in carbon trading systems.

2 Methodology

This section details the methodology employed to develop and implement an uncertainty-aware carbon flux estimation framework that integrates multispectral Landsat imagery, EC flux measurements, and ancillary environmental variables.

2.1 Dataset

We combined Landsat 8/9 Level-1 imagery with EC tower measurements and local meteorological data to train and test our deep learning model. Starting with 393 AmeriFlux BASE sites Ame (n.d.) (half-hourly flux data under the CC-BY-4.0 license), we removed sites missing key variables—wind direction (WD), carbon flux (FC), friction velocity (USTAR), wind speed (WS), air temperature (TA), relative humidity (RH), tower height(HEIGHT) and require either shortwave radiation (SW_IN) or photosynthetically active radiation (PPFD_IN), leaving 209 sites. For sites with multiple sensor measurements at the same height, we retained only the highest sensor data and averaged replicates. We further filtered out FC outliers (below the 0.5th or above the 99.5th percentile), non-physical values (e.g., negative SW_IN), and biologically implausible data (e.g., nighttime carbon drawdown without incoming radiation). Landsat scenes for each tower were downloaded via `landsatxplore` lan (n.d.) and provided 11 bands Lan (n.d.) (nine spectral at 30 m and two thermal infrared at 100 m, resampled to 30 m) along with solar and sensor azimuth/zenith angles. Each band was averaged over a 2×2 pixel window centered on the tower coordinates, which yielded the best performance in our grid search of window sizes.

2.2 Model Architecture

Our predictive model for carbon flux begins with a series of fully connected (dense) layers that transform the raw input variables into high-level features. This neural network ultimately produces outputs for a MDN Bishop (1994) layer, which parametrizes the conditional distribution of flux y given an input x. Specifically, the MDN outputs $\alpha_k(x)$, $\mu_k(x)$, and $\sigma_k^2(x)$ for $k = 1, \ldots, K$ mixture components, where $\alpha_k(x)$ are mixing coefficients, $\mu_k(x)$ the component means, and $\sigma_k^2(x)$ the component variances. The overall model thus represents the flux as a mixture of Gaussians:

$$p(y \mid x) = \sum_{k=1}^{K} \alpha_k(x)\, \mathcal{N}\big(y \mid \mu_k(x), \sigma_k^2(x)\big).$$

2.3 Uncertainty Quantification

Uncertainty in predicting carbon flux arises both from inherent noise in the data and from limitations in the model's knowledge. We follow a previously proposed method Choi et al. (2017) to decompose the total predictive uncertainty into two components: one reflecting irreducible variability in the observations (aleatoric uncertainty) and one arising from the model's limited understanding (epistemic uncertainty). Unlike Bayesian neural networks, which typically require computationally intensive Monte Carlo sampling, the method we adopted efficiently quantifies uncertainty through a single forward pass of the network.

We express the total predictive uncertainty as

$$\sigma^2_{\text{total}}(x) = \underbrace{\sum_{k=1}^{K} \alpha_k(x)\sigma_k^2(x)}_{\text{aleatoric}} + \underbrace{\sum_{k=1}^{K} \alpha_k(x) \left(\mu_k(x) - \sum_{j=1}^{K} \alpha_j(x)\mu_j(x) \right)^2}_{\text{epistemic}}$$

2.4 Training Loss

To learn the parameters θ of our network, we minimize the negative log-likelihood of the observed flux values. Given N samples $\{(x_i, y_i)\}_{i=1}^{N}$, the training objective is:

$$\mathcal{L} = -\sum_{i=1}^{N} \log \left(\sum_{k=1}^{K} \alpha_{i,k}\, \mathcal{N}\big(y_i \mid \mu_{i,k}, \sigma^2_{i,k}\big) \right),$$

where $\alpha_{i,k}$, $\mu_{i,k}$, and $\sigma^2_{i,k}$ depend on θ and are evaluated at the i-th input x_i. By training in this manner, the MDN fits a mixture model that can capture both multi-modality in carbon flux distributions and heteroscedasticity in measurement noise.

3 Results

3.1 Model Performance Across Dataset Splits and IGBP Category

The model achieves R^2 values of 0.7958, 0.7363, 0.7239, and 0.5829 on the training, validation, future test(withheld data from the last year of each training site), and site test set(withheld sites), respectively. The small drop from training to validation reflects good generalization under similar conditions, and also the further slight decrease in future test data indicates stable temporal extrapolation ability. The largest decline, observed with site test data from previously unseen towers, highlights the challenges posed by spatial heterogeneity and ecological variation. To further assess spatial variability, we grouped sites by their International Geosphere-Biosphere Programme (IGBP) vegetation categories and computed R^2 scores for the future test set. Figure 1 shows the distribution of R^2 scores across IGBP categories, revealing notable differences in model performance among land-cover types.

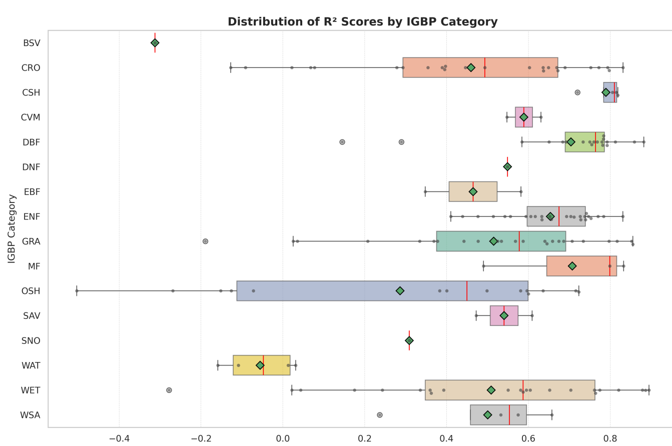

IGBP	$\mathbf{R^2}$	AU	EU
BSV	-0.3122	6.8947	1.6044
CRO	0.6698	1.5946	0.7543
CSH	0.7899	1.6778	0.6059
CVM	0.5904	0.9245	0.4504
DBF	0.7716	0.9600	0.2654
DNF	0.5491	1.4683	0.5509
EBF	0.4108	0.6323	0.3058
ENF	0.7061	1.2395	0.3810
GRA	0.6560	1.2268	0.4899
MF	0.8421	0.8286	0.1853
OSH	0.5161	2.0621	0.6658
SAV	0.5270	1.8952	0.5542
SNO	0.3090	2.0744	0.5727
WAT	0.0236	9.8240	2.0399
WET	0.7850	1.1754	0.3749
WSA	0.6248	1.5159	0.4556

Figure 1: Distribution of R^2 scores by site (left) and scaled aleatoric (AU) and epistemic uncertainty (EU) summary (right) across IGBP categories for the future test set. AU and EU are scaled by the predicted mean to allow comparison across categories.

3.2 Uncertainty Estimates and SHAP Analysis

A key contribution of this work is the decomposition of predictive uncertainty into aleatoric and epistemic components. To understand the primary drivers behind the flux predictions and the associated uncertainties, we employed SHAP(SHapley Additive exPlanations)Lundberg and Lee (2017) to compute feature contributions.

Figure 2 displays the SHAP summary plot for carbon flux predictions. The analysis reveals that features such as solar radiation (SW_IN), near-infrared reflectance (Band 5), red reflectance (Band 4 - Red), and green reflectance (Band 3 - Green) are particularly influential. This aligns with expectations, since bands 4 and 5 provide proxies of vegetation, and are often combined into a commonly used Normalized Difference Vegetation Index (NDVI).

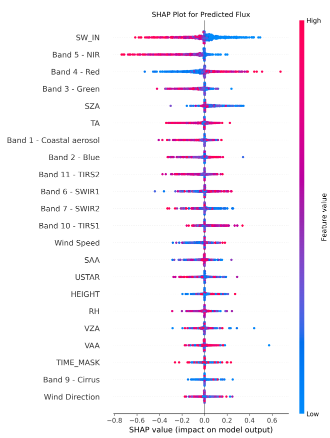

Figure 2: SHAP plot for carbon flux predictions.

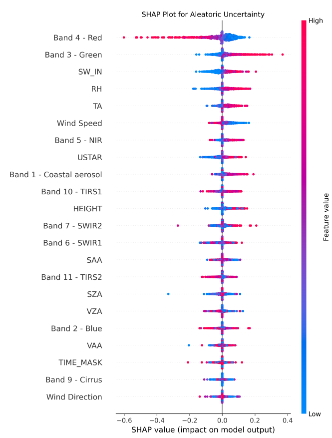

Figure 3: SHAP plot for aleatoric uncertainty.

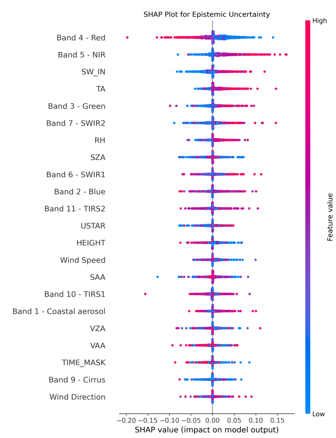

Figure 4: SHAP plot for epistemic uncertainty.

Figure 3 shows that red reflectance (Band 4 - Red), green reflectance (Band 3 - Green), solar radiation (SW_IN), relative humidity (RH), and air temperature (TA) play major roles in driving aleatoric uncertainty. These features may correspond to conditions where the model's predictions remain uncertain even with similar inputs, suggesting the presence of inherent variability in the flux response under these conditions. Similarly, Figure 4 emphasizes that features such as red reflectance (Band 4 - Red), near-infrared reflectance (Band 5), solar radiation (SW_IN), and air temperature (TA) contribute to elevated epistemic uncertainty. This indicates that the model has limited exposure to certain regions of the feature space, reducing its confidence in those predictions. These associations may help identify areas where additional data could be beneficial.

The SHAP analysis provides valuable information on the specific factors driving both the predictions and the uncertainties, offering a direction for future model refinement and targeted data acquisition efforts.

4 Conclusion and Future Work

We introduced an uncertainty-aware framework for carbon flux estimation that uses multispectral Landsat imagery, eddy covariance measurements, and auxiliary data in an MDN, explicitly separating aleatoric and epistemic uncertainties to provide insights into flux prediction model confidence. Although spatial extrapolation remains challenging, particularly in underrepresented landcover types, this work supports NCS validation and provides a better understanding of the drivers of uncertainty for remote sensing-based predictions of carbon flux. Future directions include expanding the training dataset to reduce epistemic uncertainty in poorly sampled regions and exploring Bayesian or ensemble methods for even more reliable uncertainty estimates, moving us closer to effective climate-change mitigation.

5 Acknowledgments

This material is based upon work supported by the National Science Foundation under Grant No. 2319597.

References

B. W. Griscom et al. Natural climate solutions. *Proceedings of the National Academy of Sciences*, 114(44):11645–11650, 2017.

N. Seddon et al. Understanding the value and limits of nature-based solutions to climate change and other global challenges. *Philosophical Transactions of the Royal Society B*, 375(1794):20190120, 2020.

A. Goldstein et al. Protecting irrecoverable carbon in earth's ecosystems. *Nature Climate Change*, 10:287–295, 2020.

A. R. Jacobson, J. B. Miller, A. Ballantyne, S. Basu, L. Bruhwiler, A. Chatterjee, S. Denning, and L. Ott. Chapter 8: Observations of atmospheric carbon dioxide and methane. In *Second State of the Carbon Cycle Report (SOCCR2): A Sustained Assessment Report*, pages 337–364. U.S. Global Change Research Program, 2018.

Confidence in carbon modeling, 2021. CIBO Technologies.

P. Friedlingstein et al. Global carbon budget 2023. *Earth System Science Data*, 15:5301–5369, 2023.

G. Grassi et al. Carbon fluxes from land 2000–2020: bringing clarity to countries' reporting. *Earth System Science Data*, 14:4643–4666, 2022.

D. Baldocchi et al. Assessing the eddy covariance technique for evaluating carbon dioxide exchange rates of ecosystems: past, present and future. *Global Change Biology*, 9(4): 479–492, 2003.

D. Baldocchi et al. Measuring fluxes of trace gases and energy between ecosystems and the atmosphere—the state and future of the eddy covariance method. *Global Change Biology*, 20(12):3600–3609, 2014.

G. Pastorello et al. The fluxnet2015 dataset and the oneflux processing pipeline for eddy covariance data. *Scientific Data*, 7:225, 2020.

G. P. Asner et al. High-resolution mapping of forest carbon stocks in the colombian amazon. *Biogeosciences*, 10:1383–1396, 2013.

Improved forest management (ifm) on canadian forestlands, 2021. American Carbon Registry (ACR).

D. P. Turner et al. Scaling net ecosystem production and net biome production over a heterogeneous region in the western united states. *Biogeosciences*, 4(4):597–612, 2007.

How to integrate remote sensing into the forest carbon market, the right way, 2020. American Carbon Registry (ACR).

C. Beer et al. Terrestrial gross carbon dioxide uptake: global distribution and covariation with climate. *Science*, 329(5993):834–838, 2010.

M. E. Paoletti et al. Deep learning classifiers for hyperspectral imaging: A review. *IEEE Transactions on Geoscience and Remote Sensing*, 57(9):6690–6709, 2019.

T. G. Dietterich. Ensemble methods in machine learning. In *Multiple Classifier Systems, MCS 2000, Lecture Notes in Computer Science*, volume 1857, pages 1–15. Springer, Berlin, Heidelberg, 2000.

I. Goodfellow, Y. Bengio, and A. Courville. *Deep Learning.* MIT Press, 2016.

M. Abdar et al. A review of uncertainty quantification in deep learning: Techniques, applications and challenges. *Information Fusion*, 76:243–297, 2021.

C. M. Bishop. Mixture density networks. Number NCRG/4288. 1994.

J. Choi, Z. Deng, X. Yu, and M. Chandraker. Active learning for deep object detection via probabilistic modeling. In *Proceedings of the IEEE/CVF International Conference on Computer Vision (ICCV)*, pages 10247–10256, 2021.

F. Arnez, H. Espinoza, A. Radermacher, and F. Terrier. A comparison of uncertainty estimation approaches in deep learning components for autonomous vehicle applications. arXiv preprint arXiv:2006.15172, 2020.

A. M. Saranathan et al. Assessment of advanced neural networks for the dual estimation of water quality indicators and their uncertainties. *Frontiers in Remote Sensing*, 5, 2024. Article 1383147.

C. Kirkwood, T. Economou, N. Pugeault, and H. Odbert. A deep mixture density network for outlier-corrected interpolation of crowd-sourced weather data. arXiv preprint arXiv:2201.10544, 2022.

Z. Men, E. Yee, F.-S. Lien, D. Wen, and Y. Chen. Short-term wind speed and power forecasting using an ensemble of mixture density neural networks. *Renewable Energy*, 87: 203–211, 2016.

Ameriflux base data, n.d. Available at `https://ameriflux.lbl.gov/data/`.

landsatxplore, n.d. Available at `https://github.com/yannforget/landsatxplore`.

Landsat 8/9 spectral bands, n.d. Retrieved from `https://www.usgs.gov/faqs/what-are-band-designations-landsat-satellites`.

Sungjoon Choi, Kyungjae Lee, Sungbin Lim, and Songhwai Oh. Uncertainty-aware learning from demonstration using mixture density networks with sampling-free variance modeling. *2018 IEEE International Conference on Robotics and Automation (ICRA)*, pages 6915–6922, 2017.

Scott M Lundberg and Su-In Lee. A unified approach to interpreting model predictions. In I. Guyon, U. Von Luxburg, S. Bengio, H. Wallach, R. Fergus, S. Vishwanathan, and R. Garnett, editors, *Advances in Neural Information Processing Systems*, volume 30. Curran Associates, Inc., 2017. URL `https://proceedings.neurips.cc/paper_files/paper/2017/file/8a20a8621978632d76c43dfd28b67767-Paper.pdf`.

Gabriela Posse. Ameriflux base ar-ccg carlos casares grassland, ver. 1-5. *AmeriFlux AMP*, 2022. doi: 10.17190/AMF/1865474. URL `http://doi.org/10.17190/AMF/1865474`.

Lars Kutzbach. Ameriflux base ar-tf1 rio moat bog, ver. 2-5. *AmeriFlux AMP*, 2021. doi: 10.17190/AMF/1543389. URL `http://doi.org/10.17190/AMF/1543389`.

Lars Kutzbach. Ameriflux base ar-tf2 rio pipo bog, ver. 1-5. *AmeriFlux AMP*, 2019. doi: 10.17190/AMF/1543388. URL `http://doi.org/10.17190/AMF/1543388`.

Antonio Antonino. Ameriflux base br-cst caatinga serra talhada, ver. 1-5. *AmeriFlux AMP*, 2019. doi: 10.17190/AMF/1562386. URL `http://doi.org/10.17190/AMF/1562386`.

George Vourlitis, Higo Dalmagro, José de S. Nogueira, Mark Johnson, and Paulo Arruda. Ameriflux base br-npw northern pantanal wetland, ver. 1-5. *AmeriFlux AMP*, 2019. doi: 10.17190/AMF/1579716. URL `http://doi.org/10.17190/AMF/1579716`.

Aaron Todd and Elyn Humphreys. Ameriflux base ca-arb attawapiskat river bog, ver. 1-5. *AmeriFlux AMP*, 2018a. doi: 10.17190/AMF/1480319. URL `http://doi.org/10.17190/AMF/1480319`.

Aaron Todd and Elyn Humphreys. Ameriflux base ca-arf attawapiskat river fen, ver. 1-5. *AmeriFlux AMP*, 2018b. doi: 10.17190/AMF/1480318. URL http://doi.org/10.17190/AMF/1480318.

Michelle Garneau. Ameriflux base ca-bou bouleau peatland, ver. 2-5. *AmeriFlux AMP*, 2023. doi: 10.17190/AMF/1987599. URL http://doi.org/10.17190/AMF/1987599.

Sara Knox. Ameriflux base ca-db2 delta burns bog 2, ver. 1-5. *AmeriFlux AMP*, 2021. doi: 10.17190/AMF/1811362. URL http://doi.org/10.17190/AMF/1811362.

Andreas Christen and Sara Knox. Ameriflux base ca-dbb delta burns bog, ver. 2-5. *AmeriFlux AMP*, 2021. doi: 10.17190/AMF/1543378. URL http://doi.org/10.17190/AMF/1543378.

Sara Knox. Ameriflux base ca-dsm delta salt marsh, ver. 1-5. *AmeriFlux AMP*, 2023. doi: 10.17190/AMF/1964085. URL http://doi.org/10.17190/AMF/1964085.

Claudia Wagner-Riddle. Ameriflux base ca-er1 elora research station, ver. 3-5. *AmeriFlux AMP*, 2021. doi: 10.17190/AMF/1579541. URL http://doi.org/10.17190/AMF/1579541.

Harry McCaughey. Ameriflux base ca-gro ontario - groundhog river, boreal mixedwood forest, ver. 2-5. *AmeriFlux AMP*, 2019. doi: 10.17190/AMF/1245996. URL http://doi.org/10.17190/AMF/1245996.

Thomas Andrew Black. Ameriflux base ca-lp1 british columbia - mountain pine beetle-attacked lodgepole pine stand, ver. 4-5. *AmeriFlux AMP*, 2023. doi: 10.17190/AMF/1660337. URL http://doi.org/10.17190/AMF/1660337.

M. Altaf Arain. Ameriflux base ca-tp1 ontario - turkey point 2002 plantation white pine, ver. 3-5. *AmeriFlux AMP*, 2018a. doi: 10.17190/AMF/1246009. URL http://doi.org/10.17190/AMF/1246009.

M. Altaf Arain. Ameriflux base ca-tp3 ontario - turkey point 1974 plantation white pine, ver. 3-5. *AmeriFlux AMP*, 2018b. doi: 10.17190/AMF/1246011. URL http://doi.org/10.17190/AMF/1246011.

M. Altaf Arain. Ameriflux base ca-tp4 ontario - turkey point 1939 plantation white pine, ver. 4-5. *AmeriFlux AMP*, 2018c. doi: 10.17190/AMF/1246012. URL http://doi.org/10.17190/AMF/1246012.

M. Altaf Arain. Ameriflux base ca-tpd ontario - turkey point mature deciduous, ver. 2-5. *AmeriFlux AMP*, 2018d. doi: 10.17190/AMF/1246152. URL http://doi.org/10.17190/AMF/1246152.

Jorge Perez-Quezada and Juan J. Armesto. Ameriflux base cl-sdf senda darwin forest, ver. 1-5. *AmeriFlux AMP*, 2022. doi: 10.17190/AMF/1902273. URL http://doi.org/10.17190/AMF/1902273.

Ma. Susana Alvarado-Barrientos. Ameriflux base mx-pmm puerto morelos mangrove, ver. 2-5. *AmeriFlux AMP*, 2021. doi: 10.17190/AMF/1756415. URL http://doi.org/10.17190/AMF/1756415.

Tyler Roman, Timothy Griffis, Randy Kolka, Craig Wayson, Erik Lilleskov, Dennis del Castillo Torres, Lizardo Fachin Malaverri, and Jhon Ever Rengifo Marin. Ameriflux base pe-qfr quistococha forest reserve, ver. 2-5. *AmeriFlux AMP*, 2021. doi: 10.17190/AMF/1671889. URL http://doi.org/10.17190/AMF/1671889.

NEON (National Ecological Observatory Network). Ameriflux base pr-xgu neon guanica forest (guan), ver. 6-5. *AmeriFlux AMP*, 2023a. doi: 10.17190/AMF/1773393. URL http://doi.org/10.17190/AMF/1773393.

NEON (National Ecological Observatory Network). Ameriflux base pr-xla neon lajas experimental station (laja), ver. 6-5. *AmeriFlux AMP*, 2023b. doi: 10.17190/AMF/1773394. URL `http://doi.org/10.17190/AMF/1773394`.

Dave Billesbach, Lara Kueppers, Margaret Torn, and Sebastien Biraud. Ameriflux base us-a32 arm-sgp medford hay pasture, ver. 1-5. *AmeriFlux AMP*, 2018a. doi: 10.17190/AMF/1436327. URL `http://doi.org/10.17190/AMF/1436327`.

Dave Billesbach, Lara Kueppers, Margaret Torn, and Sebastien Biraud. Ameriflux base us-a74 arm sgp milo field, ver. 1-5. *AmeriFlux AMP*, 2018b. doi: 10.17190/AMF/1436328. URL `http://doi.org/10.17190/AMF/1436328`.

Brent Olson. Ameriflux base us-alq allequash creek site, ver. 15-5. *AmeriFlux AMP*, 2023. doi: 10.17190/AMF/1480323. URL `http://doi.org/10.17190/AMF/1480323`.

Sebastien Biraud, Marc Fischer, Stephen Chan, and Margaret Torn. Ameriflux base us-arm arm southern great plains site- lamont, ver. 12-5. *AmeriFlux AMP*, 2023. doi: 10.17190/AMF/1246027. URL `http://doi.org/10.17190/AMF/1246027`.

Ray G. Anderson. Ameriflux base us-ash ussl san joaquin valley almond high salinity, ver. 1-5. *AmeriFlux AMP*, 2020a. doi: 10.17190/AMF/1634880. URL `http://doi.org/10.17190/AMF/1634880`.

Ray G. Anderson. Ameriflux base us-asl ussl san joaquin valley almond low salinity, ver. 1-5. *AmeriFlux AMP*, 2020b. doi: 10.17190/AMF/1617706. URL `http://doi.org/10.17190/AMF/1617706`.

Ray G. Anderson. Ameriflux base us-asm ussl san joaquin valley almond medium salinity, ver. 1-5. *AmeriFlux AMP*, 2020c. doi: 10.17190/AMF/1617709. URL `http://doi.org/10.17190/AMF/1617709`.

Adrian Rocha, Gaius Shaver, and John Hobbie. Ameriflux base us-an1 anaktuvuk river severe burn, ver. 2-5. *AmeriFlux AMP*, 2020a. doi: 10.17190/AMF/1246142. URL `http://doi.org/10.17190/AMF/1246142`.

Adrian Rocha, Gaius Shaver, and John Hobbie. Ameriflux base us-an2 anaktuvuk river moderate burn, ver. 2-5. *AmeriFlux AMP*, 2020b. doi: 10.17190/AMF/1246143. URL `http://doi.org/10.17190/AMF/1246143`.

Adrian Rocha, Gaius Shaver, and John Hobbie. Ameriflux base us-an3 anaktuvuk river unburned, ver. 2-5. *AmeriFlux AMP*, 2020c. doi: 10.17190/AMF/1246144. URL `http://doi.org/10.17190/AMF/1246144`.

Kimberly Novick. Ameriflux base us-brg bayles road grassland tower, ver. 1-5. *AmeriFlux AMP*, 2020. doi: 10.17190/AMF/1756416. URL `http://doi.org/10.17190/AMF/1756416`.

Eugenie Euskirchen. Ameriflux base us-bzb bonanza creek thermokarst bog, ver. 4-5. *AmeriFlux AMP*, 2022a. doi: 10.17190/AMF/1773401. URL `http://doi.org/10.17190/AMF/1773401`.

Eugenie Euskirchen. Ameriflux base us-bzf bonanza creek rich fen, ver. 4-5. *AmeriFlux AMP*, 2022b. doi: 10.17190/AMF/1756433. URL `http://doi.org/10.17190/AMF/1756433`.

Eugenie Euskirchen. Ameriflux base us-bzs bonanza creek black spruce, ver. 3-5. *AmeriFlux AMP*, 2022c. doi: 10.17190/AMF/1756434. URL `http://doi.org/10.17190/AMF/1756434`.

Eugenie Euskirchen. Ameriflux base us-bzo bonanza creek old thermokarst bog, ver. 3-5. *AmeriFlux AMP*, 2022d. doi: 10.17190/AMF/1846662. URL `http://doi.org/10.17190/AMF/1846662`.

Andrew Richardson and David Hollinger. Ameriflux base us-bar bartlett experimental forest, ver. 6-5. *AmeriFlux AMP*, 2023. doi: 10.17190/AMF/1246030. URL `http://doi.org/10.17190/AMF/1246030`.

Camilo Rey-Sanchez, Carlos Tianxin Wang, Daphne Szutu, Robert Shortt, Samuel D. Chamberlain, Joseph Verfaillie, and Dennis Baldocchi. Ameriflux base us-bi1 bouldin island alfalfa, ver. 10-5. *AmeriFlux AMP*, 2023a. doi: 10.17190/AMF/1480317. URL `http://doi.org/10.17190/AMF/1480317`.

Camilo Rey-Sanchez, Carlos Tianxin Wang, Daphne Szutu, Kyle Hemes, Joseph Verfaillie, and Dennis Baldocchi. Ameriflux base us-bi2 bouldin island corn, ver. 15-5. *AmeriFlux AMP*, 2023b. doi: 10.17190/AMF/1419513. URL `http://doi.org/10.17190/AMF/1419513`.

Claire L. Phillips and Dave Huggins. Ameriflux base us-cf1 caf-ltar cook east, ver. 3-5. *AmeriFlux AMP*, 2022. doi: 10.17190/AMF/1543382. URL `http://doi.org/10.17190/AMF/1543382`.

Dave Huggins. Ameriflux base us-cf2 caf-ltar cook west, ver. 2-5. *AmeriFlux AMP*, 2021. doi: 10.17190/AMF/1543383. URL `http://doi.org/10.17190/AMF/1543383`.

Dave Huggins. Ameriflux base us-cf3 caf-ltar boyd north, ver. 3-5. *AmeriFlux AMP*, 2022a. doi: 10.17190/AMF/1543385. URL `http://doi.org/10.17190/AMF/1543385`.

Dave Huggins. Ameriflux base us-cf4 caf-ltar boyd south, ver. 3-5. *AmeriFlux AMP*, 2022b. doi: 10.17190/AMF/1543384. URL `http://doi.org/10.17190/AMF/1543384`.

Patty Oikawa. Ameriflux base us-cgg concord grazed grassland, ver. 1-5. *AmeriFlux AMP*, 2023. doi: 10.17190/AMF/1987600. URL `http://doi.org/10.17190/AMF/1987600`.

Kenneth J. Davis. Ameriflux base us-clf cole farm, ver. 1-5. *AmeriFlux AMP*, 2023. doi: 10.17190/AMF/1987601. URL `http://doi.org/10.17190/AMF/1987601`.

Russell Scott. Ameriflux base us-cmw charleston mesquite woodland, ver. 2-5. *AmeriFlux AMP*, 2022. doi: 10.17190/AMF/1660339. URL `http://doi.org/10.17190/AMF/1660339`.

Brent Ewers, Mario Bretfeld, and Elise Pendall. Ameriflux base us-cpk chimney park, ver. 2-1. *AmeriFlux AMP*, 2016. doi: 10.17190/AMF/1246150. URL `http://doi.org/10.17190/AMF/1246150`.

Asko Noormets. Ameriflux base us-crk davy crockett national forest, ver. 2-5. *AmeriFlux AMP*, 2023. doi: 10.17190/AMF/2204055. URL `http://doi.org/10.17190/AMF/2204055`.

Jiquan Chen and Housen Chu. Ameriflux base us-crt curtice walter-berger cropland, ver. 5-5. *AmeriFlux AMP*, 2021. doi: 10.17190/AMF/1246156. URL `http://doi.org/10.17190/AMF/1246156`.

Ankur Desai. Ameriflux base us-cs1 central sands irrigated agricultural field, ver. 3-5. *AmeriFlux AMP*, 2023a. doi: 10.17190/AMF/1617710. URL `http://doi.org/10.17190/AMF/1617710`.

Ankur Desai. Ameriflux base us-cs2 tri county school pine forest, ver. 5-5. *AmeriFlux AMP*, 2023b. doi: 10.17190/AMF/1617711. URL `http://doi.org/10.17190/AMF/1617711`.

Ankur Desai. Ameriflux base us-cs3 central sands irrigated agricultural field, ver. 4-5. *AmeriFlux AMP*, 2023c. doi: 10.17190/AMF/1617713. URL `http://doi.org/10.17190/AMF/1617713`.

Ankur Desai. Ameriflux base us-cs4 central sands irrigated agricultural field, ver. 4-5. *AmeriFlux AMP*, 2023d. doi: 10.17190/AMF/1756417. URL `http://doi.org/10.17190/AMF/1756417`.

Ankur Desai. Ameriflux base us-cs5 central sands irrigated agricultural field, ver. 1-5. *AmeriFlux AMP*, 2022. doi: 10.17190/AMF/1846663. URL `http://doi.org/10.17190/AMF/1846663`.

Ankur Desai. Ameriflux base us-cs6 central sands irrigated agricultural field, ver. 1-5. *AmeriFlux AMP*, 2023e. doi: 10.17190/AMF/2001297. URL `http://doi.org/10.17190/AMF/2001297`.

Ankur Desai. Ameriflux base us-cs8 central sands irrigated agricultural field, ver. 2-5. *AmeriFlux AMP*, 2023f. doi: 10.17190/AMF/2001298. URL `http://doi.org/10.17190/AMF/2001298`.

Ken Clark. Ameriflux base us-ced cedar bridge, ver. 7-1. *AmeriFlux AMP*, 2016a. doi: 10.17190/AMF/1246043. URL `http://doi.org/10.17190/AMF/1246043`.

Alison Duff and Ankur Desai. Ameriflux base us-dfc us dairy forage research center, prairie du sac, ver. 2-5. *AmeriFlux AMP*, 2023. doi: 10.17190/AMF/1660340. URL `http://doi.org/10.17190/AMF/1660340`.

Alison Duff, Ankur Desai, and Valentin Picasso Risso. Ameriflux base us-dfk dairy forage research center - kernza, ver. 1-5. *AmeriFlux AMP*, 2021. doi: 10.17190/AMF/1825937. URL `http://doi.org/10.17190/AMF/1825937`.

Charles Ross Hinkle and Rosvel Bracho. Ameriflux base us-dpw disney wilderness preserve wetland, ver. 1-5. *AmeriFlux AMP*, 2019. doi: 10.17190/AMF/1562387. URL `http://doi.org/10.17190/AMF/1562387`.

Michael R. Schuppenhauer, Sebastien C. Biraud, Steve Deverel, and Stephen Chan. Ameriflux base us-ds3 staten rice 1, ver. 2-5. *AmeriFlux AMP*, 2023a. doi: 10.17190/AMF/1890490. URL `http://doi.org/10.17190/AMF/1890490`.

Ariane Arias-Ortiz and Dennis Baldocchi. Ameriflux base us-dmg dutch slough marsh gilbert tract, ver. 1-5. *AmeriFlux AMP*, 2023. doi: 10.17190/AMF/1964086. URL `http://doi.org/10.17190/AMF/1964086`.

Patty Oikawa. Ameriflux base us-edn eden landing ecological reserve, ver. 2-5. *AmeriFlux AMP*, 2020. doi: 10.17190/AMF/1543381. URL `http://doi.org/10.17190/AMF/1543381`.

Gregory Starr and Steve Oberbauer. Ameriflux base us-elm everglades (long hydroperiod marsh), ver. 4-1. *AmeriFlux AMP*, 2016a. doi: 10.17190/AMF/1246118. URL `http://doi.org/10.17190/AMF/1246118`.

Gregory Starr and Steve Oberbauer. Ameriflux base us-esm everglades (short hydroperiod marsh), ver. 5-1. *AmeriFlux AMP*, 2016b. doi: 10.17190/AMF/1246119. URL `http://doi.org/10.17190/AMF/1246119`.

Masahito Ueyama, Hiroki Iwata, and Yoshinobu Harazono. Ameriflux base us-fcr cascaden ridge fire scar, ver. 3-5. *AmeriFlux AMP*, 2023a. doi: 10.17190/AMF/1562388. URL `http://doi.org/10.17190/AMF/1562388`.

Chris Spence. Ameriflux base us-gl1 stannard rock, ver. 2-5. *AmeriFlux AMP*, 2023. doi: 10.17190/AMF/2204057. URL `http://doi.org/10.17190/AMF/2204057`.

John Frank and Bill Massman. Ameriflux base us-gle glees, ver. 8-5. *AmeriFlux AMP*, 2021. doi: 10.17190/AMF/1246056. URL `http://doi.org/10.17190/AMF/1246056`.

Jeremy D. Forsythe, Michael A. Kline, and Thomas L. O'Halloran. Ameriflux base us-hb1 north inlet crab haul creek, ver. 3-5. *AmeriFlux AMP*, 2023a. doi: 10.17190/AMF/1660341. URL `http://doi.org/10.17190/AMF/1660341`.

Jeremy D. Forsythe, Michael A. Kline, and Thomas L. O'Halloran. Ameriflux base us-hb2 hobcaw barony mature longleaf pine, ver. 1-5. *AmeriFlux AMP*, 2020. doi: 10.17190/AMF/1660342. URL `http://doi.org/10.17190/AMF/1660342`.

Jeremy D. Forsythe, Michael A. Kline, and Thomas L. O'Halloran. Ameriflux base us-hb3 hobcaw barony longleaf pine restoration, ver. 2-5. *AmeriFlux AMP*, 2023b. doi: 10.17190/AMF/1660343. URL http://doi.org/10.17190/AMF/1660343.

Eric Kelsey and Mark Green. Ameriflux base us-hbk hubbard brook experimental forest, ver. 2-5. *AmeriFlux AMP*, 2023. doi: 10.17190/AMF/1634881. URL http://doi.org/10.17190/AMF/1634881.

Benjamin R. K. Runkle. Ameriflux base us-hra humnoke farm rice field – field a, ver. 3-5. *AmeriFlux AMP*, 2021. doi: 10.17190/AMF/1543376. URL http://doi.org/10.17190/AMF/1543376.

Michele L. Reba. Ameriflux base us-hrc humnoke farm rice field – field c, ver. 3-5. *AmeriFlux AMP*, 2021. doi: 10.17190/AMF/1543375. URL http://doi.org/10.17190/AMF/1543375.

Heping Liu, Maoyi Huang, and Xingyuan Chen. Ameriflux base us-hn2 hanford 100h grassland, ver. 1-5. *AmeriFlux AMP*, 2019a. doi: 10.17190/AMF/1562389. URL http://doi.org/10.17190/AMF/1562389.

Heping Liu, Maoyi Huang, and Xingyuan Chen. Ameriflux base us-hn3 hanford 100h sagebrush, ver. 1-5. *AmeriFlux AMP*, 2019b. doi: 10.17190/AMF/1543379. URL http://doi.org/10.17190/AMF/1543379.

David Hollinger. Ameriflux base us-ho1 howland forest (main tower), ver. 7-5. *AmeriFlux AMP*, 2021a. doi: 10.17190/AMF/1246061. URL http://doi.org/10.17190/AMF/1246061.

David Hollinger. Ameriflux base us-ho2 howland forest (west tower), ver. 4-5. *AmeriFlux AMP*, 2021b. doi: 10.17190/AMF/1246062. URL http://doi.org/10.17190/AMF/1246062.

Ariane Arias-Ortiz, Daphne Szutu, Joseph Verfaillie, and Dennis Baldocchi. Ameriflux base us-hsm hill slough marsh, ver. 3-5. *AmeriFlux AMP*, 2023. doi: 10.17190/AMF/1890483. URL http://doi.org/10.17190/AMF/1890483.

Roser Matamala. Ameriflux base us-ib1 fermi national accelerator laboratory- batavia (agricultural site), ver. 8-5. *AmeriFlux AMP*, 2019a. doi: 10.17190/AMF/1246065. URL http://doi.org/10.17190/AMF/1246065.

Roser Matamala. Ameriflux base us-ib2 fermi national accelerator laboratory- batavia (prairie site), ver. 8-5. *AmeriFlux AMP*, 2019b. doi: 10.17190/AMF/1246066. URL http://doi.org/10.17190/AMF/1246066.

Eugenie Euskirchen, Gaius Shaver, and Syndonia Bret-Harte. Ameriflux base us-ich imnavait creek watershed heath tundra, ver. 4-5. *AmeriFlux AMP*, 2022a. doi: 10.17190/AMF/1246133. URL http://doi.org/10.17190/AMF/1246133.

Eugenie Euskirchen, Gaius Shaver, and Syndonia Bret-Harte. Ameriflux base us-ics imnavait creek watershed wet sedge tundra, ver. 7-5. *AmeriFlux AMP*, 2022b. doi: 10.17190/AMF/1246130. URL http://doi.org/10.17190/AMF/1246130.

Eugenie Euskirchen, Gaius Shaver, and Syndonia Bret-Harte. Ameriflux base us-ict imnavait creek watershed tussock tundra, ver. 5-5. *AmeriFlux AMP*, 2022c. doi: 10.17190/AMF/1246131. URL http://doi.org/10.17190/AMF/1246131.

Enrique R. Vivoni and Eli R. Perez-Ruiz. Ameriflux base us-jo2 jornada experimental range mixed shrubland, ver. 2-5. *AmeriFlux AMP*, 2022. doi: 10.17190/AMF/1617696. URL http://doi.org/10.17190/AMF/1617696.

Nathaniel Brunsell. Ameriflux base us-kfs kansas field station, ver. 7-5. *AmeriFlux AMP*, 2020a. doi: 10.17190/AMF/1246132. URL http://doi.org/10.17190/AMF/1246132.

Nathaniel Brunsell. Ameriflux base us-kls kansas land institute, ver. 2-5. *AmeriFlux AMP*, 2021. doi: 10.17190/AMF/1498745. URL http://doi.org/10.17190/AMF/1498745.

Patrick Sullivan. Ameriflux base us-kpl lily lake fen, ver. 2-5. *AmeriFlux AMP*, 2023. doi: 10.17190/AMF/1865478. URL http://doi.org/10.17190/AMF/1865478.

Rosvel Bracho and Charles Ross Hinkle. Ameriflux base us-ks3 kennedy space center (salt marsh), ver. 1-5. *AmeriFlux AMP*, 2019. doi: 10.17190/AMF/1562390. URL http://doi.org/10.17190/AMF/1562390.

Nathaniel Brunsell. Ameriflux base us-kon konza prairie lter (knz), ver. 5-5. *AmeriFlux AMP*, 2020b. doi: 10.17190/AMF/1246068. URL http://doi.org/10.17190/AMF/1246068.

Jeffrey Wood and Lianhong Gu. Ameriflux base us-moz missouri ozark site, ver. 11-5. *AmeriFlux AMP*, 2022. doi: 10.17190/AMF/1246081. URL http://doi.org/10.17190/AMF/1246081.

Bev Law. Ameriflux base us-me2 metolius mature ponderosa pine, ver. 18-5. *AmeriFlux AMP*, 2022. doi: 10.17190/AMF/1246076. URL http://doi.org/10.17190/AMF/1246076.

Bev Law. Ameriflux base us-me6 metolius young pine burn, ver. 16-5. *AmeriFlux AMP*, 2023. doi: 10.17190/AMF/1246128. URL http://doi.org/10.17190/AMF/1246128.

Ankur Desai. Ameriflux base us-men lake mendota, center for limnology site, ver. 3-5. *AmeriFlux AMP*, 2018. doi: 10.17190/AMF/1433375. URL http://doi.org/10.17190/AMF/1433375.

Adam Schreiner-McGraw. Ameriflux base us-mo1 ltar cmrb field 1 (cmrb asp), ver. 2-5. *AmeriFlux AMP*, 2023a. doi: 10.17190/AMF/1870588. URL http://doi.org/10.17190/AMF/1870588.

Adam Schreiner-McGraw. Ameriflux base us-mo2 ltar cmrb tucker prairie (cmrb tp), ver. 2-5. *AmeriFlux AMP*, 2023b. doi: 10.17190/AMF/1902276. URL http://doi.org/10.17190/AMF/1902276.

Adam Schreiner-McGraw. Ameriflux base us-mo3 ltar cmrb field 3 (cmrb bau), ver. 2-5. *AmeriFlux AMP*, 2023c. doi: 10.17190/AMF/1870589. URL http://doi.org/10.17190/AMF/1870589.

Marcy Litvak. Ameriflux base us-mpj mountainair pinyon-juniper woodland, ver. 22-5. *AmeriFlux AMP*, 2023a. doi: 10.17190/AMF/1246123. URL http://doi.org/10.17190/AMF/1246123.

Jaclyn Hatala Matthes, Cove Sturtevant, Patty Oikawa, Samuel D Chamberlain, Daphne Szutu, Ariane Arias-Ortiz, Joseph Verfaillie, and Dennis Baldocchi. Ameriflux base us-myb mayberry wetland, ver. 13-5. *AmeriFlux AMP*, 2022. doi: 10.17190/AMF/1246139. URL http://doi.org/10.17190/AMF/1246139.

Asko Noormets, Ge Sun, Michael Gavazzi, Jean-Christophe Domec, Steve McNulty, Guofang Miao, Maricar Aguilos, Bhaskar Mitra, Kevan Minick, John King, Linqing Yang, and Prajaya Prajapati. Ameriflux base us-nc2 nc_loblolly plantation, ver. 11-5. *AmeriFlux AMP*, 2023. doi: 10.17190/AMF/1246083. URL http://doi.org/10.17190/AMF/1246083.

Asko Noormets, Michael Gavazzi, Maricar Aguilos, John King, Bhaskar Mitra, and Jean-Christophe Domec. Ameriflux base us-nc3 nc_clearcut#3, ver. 4-5. *AmeriFlux AMP*, 2022a. doi: 10.17190/AMF/1419506. URL http://doi.org/10.17190/AMF/1419506.

Asko Noormets, John King, Bhaskar Mitra, Guofang Miao, Maricar Aguilos, Kevan Minick, Prajaya Prajapati, and Jean-Christophe Domec. Ameriflux base us-nc4 nc_alligatorriver, ver. 5-5. *AmeriFlux AMP*, 2022b. doi: 10.17190/AMF/1480314. URL http://doi.org/10.17190/AMF/1480314.

Margaret Torn and Sigrid Dengel. Ameriflux base us-ngb ngee arctic barrow, ver. 5-5. *AmeriFlux AMP*, 2023a. doi: 10.17190/AMF/1436326. URL http://doi.org/10.17190/AMF/1436326.

Margaret Torn and Sigrid Dengel. Ameriflux base us-ngc ngee arctic council, ver. 3-5. *AmeriFlux AMP*, 2023b. doi: 10.17190/AMF/1634883. URL http://doi.org/10.17190/AMF/1634883.

Peter D. Blanken, Russel K. Monson, Sean P. Burns, David R. Bowling, and Andrew A. Turnipseed. Ameriflux base us-nr1 niwot ridge forest (lter nwt1), ver. 20-5. *AmeriFlux AMP*, 2023. doi: 10.17190/AMF/1246088. URL http://doi.org/10.17190/AMF/1246088.

John Knowles. Ameriflux base us-nr3 niwot ridge alpine (t-van west), ver. 4-5. *AmeriFlux AMP*, 2023a. doi: 10.17190/AMF/1804491. URL http://doi.org/10.17190/AMF/1804491.

John Knowles. Ameriflux base us-nr4 niwot ridge alpine (t-van east), ver. 4-5. *AmeriFlux AMP*, 2023b. doi: 10.17190/AMF/1804492. URL http://doi.org/10.17190/AMF/1804492.

Maria L. Silveira and Rosvel Bracho. Ameriflux base us-ona florida pine flatwoods, ver. 3-5. *AmeriFlux AMP*, 2022. doi: 10.17190/AMF/1660350. URL http://doi.org/10.17190/AMF/1660350.

Gil Bohrer. Ameriflux base us-orv olentangy river wetland research park, ver. 3-5. *AmeriFlux AMP*, 2020. doi: 10.17190/AMF/1246135. URL http://doi.org/10.17190/AMF/1246135.

Gil Bohrer and Janice Kerns. Ameriflux base us-owc old woman creek, ver. 4-5. *AmeriFlux AMP*, 2023. doi: 10.17190/AMF/1418679. URL http://doi.org/10.17190/AMF/1418679.

Jiquan Chen, Housen Chu, and Asko Noormets. Ameriflux base us-oho oak openings, ver. 7-5. *AmeriFlux AMP*, 2021. doi: 10.17190/AMF/1246089. URL http://doi.org/10.17190/AMF/1246089.

Ray G. Anderson. Ameriflux base us-psh ussl san joaquin valley pistachio high, ver. 1-5. *AmeriFlux AMP*, 2020d. doi: 10.17190/AMF/1617719. URL http://doi.org/10.17190/AMF/1617719.

Ray G. Anderson. Ameriflux base us-psl ussl san joaquin valley pistachio low, ver. 1-5. *AmeriFlux AMP*, 2020e. doi: 10.17190/AMF/1617720. URL http://doi.org/10.17190/AMF/1617720.

Ankur Desai. Ameriflux base us-pnp lake mendota, picnic point site, ver. 8-5. *AmeriFlux AMP*, 2023g. doi: 10.17190/AMF/1433376. URL http://doi.org/10.17190/AMF/1433376.

Go Iwahana, Hideki Kobayashi, Hiroki Ikawa, and Rikie Suzuki. Ameriflux base us-prr poker flat research range black spruce forest, ver. 4-5. *AmeriFlux AMP*, 2023. doi: 10.17190/AMF/1246153. URL http://doi.org/10.17190/AMF/1246153.

Michael R. Schuppenhauer, Sebastien C. Biraud, and Stephen Chan. Ameriflux base us-rga arkansas corn farm, ver. 3-5. *AmeriFlux AMP*, 2023b. doi: 10.17190/AMF/1880913. URL http://doi.org/10.17190/AMF/1880913.

Michael Schuppenhauer, Sebastien C. Biraud, and Stephen Chan. Ameriflux base us-rgb butte county rice farm, ver. 4-5. *AmeriFlux AMP*, 2023c. doi: 10.17190/AMF/1870591. URL http://doi.org/10.17190/AMF/1870591.

Michael R. Schuppenhauer, Sebastien C. Biraud, and Stephen Chan. Ameriflux base us-rgf stanislaus county forage farm, ver. 1-5. *AmeriFlux AMP*, 2023d. doi: 10.17190/AMF/2001310. URL http://doi.org/10.17190/AMF/2001310.

Michael R. Schuppenhauer, Sebastien C. Biraud, and Stephen Chan. Ameriflux base us-rgw desha county rice farm, ver. 3-5. *AmeriFlux AMP*, 2023e. doi: 10.17190/AMF/1880915. URL http://doi.org/10.17190/AMF/1880915.

Michael R. Schuppenhauer, Sebastien C. Biraud, and Stephen Chan. Ameriflux base us-rgo glenn county organic rice farm, ver. 3-5. *AmeriFlux AMP*, 2023f. doi: 10.17190/AMF/1880914. URL http://doi.org/10.17190/AMF/1880914.

Gerald Flerchinger. Ameriflux base us-rls rcew low sagebrush, ver. 5-5. *AmeriFlux AMP*, 2023a. doi: 10.17190/AMF/1418682. URL http://doi.org/10.17190/AMF/1418682.

Gerald Flerchinger. Ameriflux base us-rms rcew mountain big sagebrush, ver. 5-5. *AmeriFlux AMP*, 2023b. doi: 10.17190/AMF/1375202. URL http://doi.org/10.17190/AMF/1375202.

John Baker, Tim Griffis, and Timothy Griffis. Ameriflux base us-ro1 rosemount- g21, ver. 5-5. *AmeriFlux AMP*, 2018. doi: 10.17190/AMF/1246092. URL http://doi.org/10.17190/AMF/1246092.

John Baker and Tim Griffis. Ameriflux base us-ro2 rosemount- c7, ver. 2-5. *AmeriFlux AMP*, 2023a. doi: 10.17190/AMF/1418683. URL http://doi.org/10.17190/AMF/1418683.

John Baker and Tim Griffis. Ameriflux base us-ro4 rosemount prairie, ver. 22-5. *AmeriFlux AMP*, 2023b. doi: 10.17190/AMF/1419507. URL http://doi.org/10.17190/AMF/1419507.

John Baker and Tim Griffis. Ameriflux base us-ro5 rosemount i18$_south, ver. 22 - 5. AmeriFlux\ AMP, 2023c. doi:.$ URL http://doi.org/10.17190/AMF/1419508.

John Baker and Tim Griffis. Ameriflux base us-ro6 rosemount i18$_north, ver. 22 - 5. AmeriFlux\ AMP, 2023d. 10.17190/AMF/1419509. URL.$

Masahito Ueyama, Hiroki Iwata, and Yoshinobu Harazono. Ameriflux base us-rpf poker flat research range: Succession from fire scar to deciduous forest, ver. 9-5. *AmeriFlux AMP*, 2023b. 10.17190/AMF/1579540. URL http://doi.org/10.17190/AMF/1579540.

Gerald Flerchinger. Ameriflux base us-rwf rcew upper sheep prescibed fire, ver. 3-5. *AmeriFlux AMP*, 2023c. 10.17190/AMF/1617724. URL http://doi.org/10.17190/AMF/1617724.

Gerald Flerchinger. Ameriflux base us-rws reynolds creek wyoming big sagebrush, ver. 5-5. *AmeriFlux AMP*, 2023d. 10.17190/AMF/1375201. URL http://doi.org/10.17190/AMF/1375201.

Rosvel Bracho and Timothy A. Martin. Ameriflux base us-sp1 slashpine-austin cary- 65yrs nat regen, ver. 5-5. *AmeriFlux AMP*, 2023. 10.17190/AMF/1246100. URL http://doi.org/10.17190/AMF/1246100.

Shirley Kurc. Ameriflux base us-src santa rita creosote, ver. 6-5. *AmeriFlux AMP*, 2019. 10.17190/AMF/1246127. URL http://doi.org/10.17190/AMF/1246127.

Russell Scott. Ameriflux base us-srg santa rita grassland, ver. 15-5. *AmeriFlux AMP*, 2023a. 10.17190/AMF/1246154. URL http://doi.org/10.17190/AMF/1246154.

Russell Scott. Ameriflux base us-srm santa rita mesquite, ver. 26-5. *AmeriFlux AMP*, 2023b. 10.17190/AMF/1246104. URL http://doi.org/10.17190/AMF/1246104.

Enrique R. Vivoni. Ameriflux base us-srs santa rita savanna, ver. 3-5. *AmeriFlux AMP*, 2022. 10.17190/AMF/1660351. URL http://doi.org/10.17190/AMF/1660351.

Brandon R. Forsythe, Jason Horne, and Kenneth J. Davis. Ameriflux base us-ssh susquehanna shale hills critical zone observatory, ver. 1-5. *AmeriFlux AMP*, 2022. 10.17190/AMF/1880916. URL http://doi.org/10.17190/AMF/1880916.

Marcy Litvak. Ameriflux base us-seg sevilleta grassland, ver. 23-5. *AmeriFlux AMP*, 2023b. 10.17190/AMF/1246124. URL http://doi.org/10.17190/AMF/1246124.

Marcy Litvak. Ameriflux base us-ses sevilleta shrubland, ver. 22-5. *AmeriFlux AMP*, 2023c. 10.17190/AMF/1246125. URL http://doi.org/10.17190/AMF/1246125.

Ken Clark. Ameriflux base us-slt silas little- new jersey, ver. 5-1. *AmeriFlux AMP*, 2016b. 10.17190/AMF/1246096. URL http://doi.org/10.17190/AMF/1246096.

Matteo Detto, Cove Sturtevant, Patty Oikawa, Joseph Verfaillie, and Dennis Baldocchi. Ameriflux base us-snd sherman island, ver. 2-1. *AmeriFlux AMP*, 2016. 10.17190/AMF/1246094. URL http://doi.org/10.17190/AMF/1246094.

Robert Shortt, Kyle Hemes, Daphne Szutu, Joseph Verfaillie, and Dennis Baldocchi. Ameriflux base us-sne sherman island restored wetland, ver. 7-5. *AmeriFlux AMP*, 2021. 10.17190/AMF/1418684. URL http://doi.org/10.17190/AMF/1418684.

Kuno Kusak, Camilo Rey Sanchez, Daphne Szutu, and Dennis Baldocchi. Ameriflux base us-snf sherman barn, ver. 3-5. *AmeriFlux AMP*, 2020. 10.17190/AMF/1579718. URL http://doi.org/10.17190/AMF/1579718.

Brian Bergamaschi and Lisamarie Windham-Myers. Ameriflux base us-srr suisun marsh - rush ranch, ver. 1-5. *AmeriFlux AMP*, 2018. 10.17190/AMF/1418685. URL http://doi.org/10.17190/AMF/1418685.

Rodrigo Vargas. Ameriflux base us-stj st jones reserve, ver. 2-5. *AmeriFlux AMP*, 2020. 10.17190/AMF/1480316. URL http://doi.org/10.17190/AMF/1480316.

Ankur Desai. Ameriflux base us-syv sylvania wilderness area, ver. 26-5. *AmeriFlux AMP*, 2023h. 10.17190/AMF/1246106. URL http://doi.org/10.17190/AMF/1246106.

Alex Valach, Robert Shortt, Daphne Szutu, Elke Eichelmann, Sara Knox, Kyle Hemes, Joseph Verfaillie, and Dennis Baldocchi. Ameriflux base us-tw1 twitchell wetland west pond, ver. 10-5. *AmeriFlux AMP*, 2023. 10.17190/AMF/1246147. URL http://doi.org/10.17190/AMF/1246147.

Cove Sturtevant, Joseph Verfaillie, and Dennis Baldocchi. Ameriflux base us-tw2 twitchell corn, ver. 2-5. *AmeriFlux AMP*, 2019. 10.17190/AMF/1246148. URL http://doi.org/10.17190/AMF/1246148.

Samuel D Chamberlain, Patty Oikawa, Cove Sturtevant, Daphne Szutu, Joseph Verfaillie, and Dennis Baldocchi. Ameriflux base us-tw3 twitchell alfalfa, ver. 5-5. *AmeriFlux AMP*, 2018. 10.17190/AMF/1246149. URL http://doi.org/10.17190/AMF/1246149.

Elke Eichelmann, Robert Shortt, Sara Knox, Camilo Rey Sanchez, Alex Valach, Cove Sturtevant, Daphne Szutu, Joseph Verfaillie, and Dennis Baldocchi. Ameriflux base us-tw4 twitchell east end wetland, ver. 13-5. *AmeriFlux AMP*, 2023. 10.17190/AMF/1246151. URL http://doi.org/10.17190/AMF/1246151.

Alex Valach, Kuno Kasak, Daphne Szutu, Joseph Verfaillie, and Dennis Baldocchi. Ameriflux base us-tw5 east pond wetland, ver. 3-5. *AmeriFlux AMP*, 2020. 10.17190/AMF/1543380. URL http://doi.org/10.17190/AMF/1543380.

Sara Knox, Jaclyn Hatala Matthes, Joseph Verfaillie, and Dennis Baldocchi. Ameriflux base us-twt twitchell island, ver. 7-5. *AmeriFlux AMP*, 2023. 10.17190/AMF/1246140. URL http://doi.org/10.17190/AMF/1246140.

Gil Bohrer. Ameriflux base us-um3 douglas lake, ver. 1-5. *AmeriFlux AMP*, 2018. 10.17190/AMF/1480315. URL http://doi.org/10.17190/AMF/1480315.

Christopher Gough, Gil Bohrer, and Peter Curtis. Ameriflux base us-umb univ. of mich. biological station, ver. 20-5. *AmeriFlux AMP*, 2023. 10.17190/AMF/1246107. URL http://doi.org/10.17190/AMF/1246107.

Kathryn Ladig and Paul Inkenbrandt. Ameriflux base us-utb uflux bonneville salt flats, ver. 1-5. *AmeriFlux AMP*, 2023. 10.17190/AMF/2001311. URL http://doi.org/10.17190/AMF/2001311.

Masahito Ueyama, Hiroki Iwata, and Yoshinobu Harazono. Ameriflux base us-uaf university of alaska, fairbanks, ver. 11-5. *AmeriFlux AMP*, 2023c. 10.17190/AMF/1480322. URL http://doi.org/10.17190/AMF/1480322.

Siyan Ma, Liukang Xu, Joseph Verfaillie, and Dennis Baldocchi. Ameriflux base us-var vaira ranch- ione, ver. 19-5. *AmeriFlux AMP*, 2023. 10.17190/AMF/1245984. URL http://doi.org/10.17190/AMF/1245984.

Marcy Litvak. Ameriflux base us-vcm valles caldera mixed conifer, ver. 24-5. *AmeriFlux AMP*, 2023d. 10.17190/AMF/1246121. URL http://doi.org/10.17190/AMF/1246121.

Marcy Litvak. Ameriflux base us-vcp valles caldera ponderosa pine, ver. 22-5. *AmeriFlux AMP*, 2023e. 10.17190/AMF/1246122. URL http://doi.org/10.17190/AMF/1246122.

Marcy Litvak. Ameriflux base us-vcs valles caldera sulphur springs mixed conifer, ver. 14-5. *AmeriFlux AMP*, 2023f. 10.17190/AMF/1418681. URL http://doi.org/10.17190/AMF/1418681.

Jiquan Chen and Housen Chu. Ameriflux base us-wpt winous point north marsh, ver. 4-5. *AmeriFlux AMP*, 2019. 10.17190/AMF/1246155. URL http://doi.org/10.17190/AMF/1246155.

Russ Scott. Ameriflux base us-whs walnut gulch lucky hills shrub, ver. 21-5. *AmeriFlux AMP*, 2023c. 10.17190/AMF/1246113. URL http://doi.org/10.17190/AMF/1246113.

Marcy Litvak. Ameriflux base us-wjs willard juniper savannah, ver. 22-5. *AmeriFlux AMP*, 2023g. 10.17190/AMF/1246120. URL http://doi.org/10.17190/AMF/1246120.

Russell Scott. Ameriflux base us-wkg walnut gulch kendall grasslands, ver. 21-5. *AmeriFlux AMP*, 2023d. 10.17190/AMF/1246112. URL http://doi.org/10.17190/AMF/1246112.

Sonia Wharton. Ameriflux base us-wrc wind river crane site, ver. 8-1. *AmeriFlux AMP*, 2016. 10.17190/AMF/1246114. URL http://doi.org/10.17190/AMF/1246114.

NEON (National Ecological Observatory Network). Ameriflux base us-xab neon abby road (abby), ver. 8-5. *AmeriFlux AMP*, 2023c. 10.17190/AMF/1617726. URL http://doi.org/10.17190/AMF/1617726.

NEON (National Ecological Observatory Network). Ameriflux base us-xae neon klemme range research station (oaes), ver. 7-5. *AmeriFlux AMP*, 2023d. 10.17190/AMF/1671891. URL http://doi.org/10.17190/AMF/1671891.

NEON (National Ecological Observatory Network). Ameriflux base us-xba neon barrow environmental observatory (barr), ver. 7-5. *AmeriFlux AMP*, 2023e. 10.17190/AMF/1671892. URL http://doi.org/10.17190/AMF/1671892.

NEON (National Ecological Observatory Network). Ameriflux base us-xbl neon blandy experimental farm (blan), ver. 7-5. *AmeriFlux AMP*, 2023f. 10.17190/AMF/1671893. URL http://doi.org/10.17190/AMF/1671893.

NEON (National Ecological Observatory Network). Ameriflux base us-xbn neon caribou creek - poker flats watershed (bona), ver. 8-5. *AmeriFlux AMP*, 2023g. 10.17190/AMF/1617727. URL http://doi.org/10.17190/AMF/1617727.

NEON (National Ecological Observatory Network). Ameriflux base us-xbr neon bartlett experimental forest (bart), ver. 8-5. *AmeriFlux AMP*, 2023h. 10.17190/AMF/1579542. URL http://doi.org/10.17190/AMF/1579542.

NEON (National Ecological Observatory Network). Ameriflux base us-xcl neon lbj national grassland (clbj), ver. 7-5. *AmeriFlux AMP*, 2023i. 10.17190/AMF/1671894. URL http://doi.org/10.17190/AMF/1671894.

NEON (National Ecological Observatory Network). Ameriflux base us-xcp neon central plains experimental range (cper), ver. 8-5. *AmeriFlux AMP*, 2023j. 10.17190/AMF/1579720. URL http://doi.org/10.17190/AMF/1579720.

NEON (National Ecological Observatory Network). Ameriflux base us-xdc neon dakota coteau field school (dcfs), ver. 8-5. *AmeriFlux AMP*, 2023k. 10.17190/AMF/1617728. URL http://doi.org/10.17190/AMF/1617728.

NEON (National Ecological Observatory Network). Ameriflux base us-xdj neon delta junction (deju), ver. 8-5. *AmeriFlux AMP*, 2023l. 10.17190/AMF/1634884. URL http://doi.org/10.17190/AMF/1634884.

NEON (National Ecological Observatory Network). Ameriflux base us-xdl neon dead lake (dela), ver. 8-5. *AmeriFlux AMP*, 2023m. 10.17190/AMF/1579721. URL http://doi.org/10.17190/AMF/1579721.

NEON (National Ecological Observatory Network). Ameriflux base us-xds neon disney wilderness preserve (dsny), ver. 7-5. *AmeriFlux AMP*, 2023n. 10.17190/AMF/1671895. URL http://doi.org/10.17190/AMF/1671895.

NEON (National Ecological Observatory Network). Ameriflux base us-xgr neon great smoky mountains national park, twin creeks (grsm), ver. 8-5. *AmeriFlux AMP*, 2023o. 10.17190/AMF/1634885. URL http://doi.org/10.17190/AMF/1634885.

NEON (National Ecological Observatory Network). Ameriflux base us-xha neon harvard forest (harv), ver. 9-5. *AmeriFlux AMP*, 2023p. 10.17190/AMF/1562391. URL http://doi.org/10.17190/AMF/1562391.

NEON (National Ecological Observatory Network). Ameriflux base us-xhe neon healy (heal), ver. 8-5. *AmeriFlux AMP*, 2023q. 10.17190/AMF/1617729. URL http://doi.org/10.17190/AMF/1617729.

NEON (National Ecological Observatory Network). Ameriflux base us-xje neon jones ecological research center (jerc), ver. 8-5. *AmeriFlux AMP*, 2023r. 10.17190/AMF/1617730. URL http://doi.org/10.17190/AMF/1617730.

NEON (National Ecological Observatory Network). Ameriflux base us-xjr neon jornada lter (jorn), ver. 8-5. *AmeriFlux AMP*, 2023s. 10.17190/AMF/1617731. URL http://doi.org/10.17190/AMF/1617731.

NEON (National Ecological Observatory Network). Ameriflux base us-xka neon konza prairie biological station - relocatable (kona), ver. 8-5. *AmeriFlux AMP*, 2023t. 10.17190/AMF/1579722. URL http://doi.org/10.17190/AMF/1579722.

NEON (National Ecological Observatory Network). Ameriflux base us-xkz neon konza prairie biological station (konz), ver. 9-5. *AmeriFlux AMP*, 2023u. 10.17190/AMF/1562392. URL http://doi.org/10.17190/AMF/1562392.

NEON (National Ecological Observatory Network). Ameriflux base us-xle neon lenoir landing (leno), ver. 6-5. *AmeriFlux AMP*, 2023v. 10.17190/AMF/1773398. URL http://doi.org/10.17190/AMF/1773398.

NEON (National Ecological Observatory Network). Ameriflux base us-xmb neon moab (moab), ver. 7-5. *AmeriFlux AMP*, 2023w. 10.17190/AMF/1671896. URL http://doi.org/10.17190/AMF/1671896.

NEON (National Ecological Observatory Network). Ameriflux base us-xml neon mountain lake biological station (mlbs), ver. 7-5. *AmeriFlux AMP*, 2023x. 10.17190/AMF/1671897. URL http://doi.org/10.17190/AMF/1671897.

NEON (National Ecological Observatory Network). Ameriflux base us-xng neon northern great plains research laboratory (nogp), ver. 8-5. *AmeriFlux AMP*, 2023y. 10.17190/AMF/1617732. URL http://doi.org/10.17190/AMF/1617732.

NEON (National Ecological Observatory Network). Ameriflux base us-xnq neon onaquiault (onaq), ver. 8-5. *AmeriFlux AMP*, 2023z. 10.17190/AMF/1617733. URL http://doi.org/10.17190/AMF/1617733.

NEON (National Ecological Observatory Network). Ameriflux base us-xrm neon rocky mountain national park, castnet (rmnp), ver. 8-5. *AmeriFlux AMP*, 2023—. 10.17190/AMF/1579723. URL http://doi.org/10.17190/AMF/1579723.

)]US-xRN NEON (National Ecological Observatory Network). Ameriflux base us-xrn neon oak ridge national lab (ornl), ver. 6-5. *AmeriFlux AMP*, 2023. 10.17190/AMF/1773400. URL http://doi.org/10.17190/AMF/1773400.

NEON (National Ecological Observatory Network). Ameriflux base us-xsb neon ordway-swisher biological station (osbs), ver. 7-5. *AmeriFlux AMP*, 2023 . 10.17190/AMF/1671899. URL http://doi.org/10.17190/AMF/1671899.

NEON (National Ecological Observatory Network). Ameriflux base us-xsc neon smithsonian conservation biology institute (scbi), ver. 7-5. *AmeriFlux AMP*, 2023. 10.17190/AMF/1671900. URL http://doi.org/10.17190/AMF/1671900.

NEON (National Ecological Observatory Network). Ameriflux base us-xse neon smithsonian environmental research center (serc), ver. 8-5. *AmeriFlux AMP*, 2023. 10.17190/AMF/1617734. URL http://doi.org/10.17190/AMF/1617734.

NEON (National Ecological Observatory Network). Ameriflux base us-xsj neon san joaquin experimental range (sjer), ver. 7-5. *AmeriFlux AMP*, 2023. 10.17190/AMF/1671901. URL http://doi.org/10.17190/AMF/1671901.

NEON (National Ecological Observatory Network). Ameriflux base us-xsl neon north sterling, co (ster), ver. 8-5. *AmeriFlux AMP*, 2023. 10.17190/AMF/1617735. URL http://doi.org/10.17190/AMF/1617735.

NEON (National Ecological Observatory Network). Ameriflux base us-xsp neon soaproot saddle (soap), ver. 8-5. *AmeriFlux AMP*, 2023. 10.17190/AMF/1617736. URL http://doi.org/10.17190/AMF/1617736.

NEON (National Ecological Observatory Network). Ameriflux base us-xsr neon santa rita experimental range (srer), ver. 8-5. *AmeriFlux AMP*, 2023. 10.17190/AMF/1579543. URL http://doi.org/10.17190/AMF/1579543.

NEON (National Ecological Observatory Network). Ameriflux base us-xst neon steigerwaldt land services (stei), ver. 8-5. *AmeriFlux AMP*, 2023. 10.17190/AMF/1617737. URL http://doi.org/10.17190/AMF/1617737.

NEON (National Ecological Observatory Network). Ameriflux base us-xta neon talladega national forest (tall), ver. 7-5. *AmeriFlux AMP*, 2023. 10.17190/AMF/1671902. URL http://doi.org/10.17190/AMF/1671902.

NEON (National Ecological Observatory Network). Ameriflux base us-xtl neon toolik (tool), ver. 8-5. *AmeriFlux AMP*, 2023. 10.17190/AMF/1617739. URL http://doi.org/10.17190/AMF/1617739.

NEON (National Ecological Observatory Network). Ameriflux base us-xtr neon treehaven (tree), ver. 8-5. *AmeriFlux AMP*, 2023. 10.17190/AMF/1634886. URL http://doi.org/10.17190/AMF/1634886.

NEON (National Ecological Observatory Network). Ameriflux base us-xuk neon the university of kansas field station (ukfs), ver. 8-5. *AmeriFlux AMP*, 2023. 10.17190/AMF/1617740. URL http://doi.org/10.17190/AMF/1617740.

NEON (National Ecological Observatory Network). Ameriflux base us-xun neon university of notre dame environmental research center (unde), ver. 8-5. *AmeriFlux AMP*, 2023. 10.17190/AMF/1617741. URL `http://doi.org/10.17190/AMF/1617741`.

NEON (National Ecological Observatory Network). Ameriflux base us-xwd neon woodworth (wood), ver. 8-5. *AmeriFlux AMP*, 2023. 10.17190/AMF/1579724. URL `http://doi.org/10.17190/AMF/1579724`.

NEON (National Ecological Observatory Network). Ameriflux base us-xwr neon wind river experimental forest (wref), ver. 8-5. *AmeriFlux AMP*, 2023. 10.17190/AMF/1617742. URL `http://doi.org/10.17190/AMF/1617742`.

NEON (National Ecological Observatory Network). Ameriflux base us-xye neon yellowstone northern range (frog rock) (yell), ver. 8-5. *AmeriFlux AMP*, 2023. 10.17190/AMF/1617743. URL `http://doi.org/10.17190/AMF/1617743`.

Appendices

A Additional Results

A.1 Future Test Set Performance by IGBP Category

Table 1: Future Test Set Performance by IGBP Category. The Future Test Set contains observations collected at later timestamps than those in the training/validation sets, assessing the model's capacity to predict fluxes forward in time.

IGBP	R^2	AU	AU Scaled	EU	EU Scaled	Pred	True	RMSE
BSV	-0.3122	1.0224	6.8947	0.2379	1.6044	0.1483	-0.3785	1.2686
CRO	0.6698	1.9139	1.5946	0.9053	0.7543	-1.2002	-1.3431	3.3006
CSH	0.7899	1.4169	1.6778	0.5117	0.6059	-0.8445	-1.2777	2.2382
CVM	0.5904	2.6260	0.9245	1.2793	0.4504	-2.8405	-2.8789	3.2751
DBF	0.7716	2.7724	0.9600	0.7665	0.2654	-2.8879	-2.7674	3.3202
DNF	0.5491	3.1512	1.4683	1.1823	0.5509	-2.1462	-2.0343	3.2492
EBF	0.4108	3.4776	0.6323	1.6819	0.3058	-5.5003	-4.1669	4.0152
ENF	0.7061	2.1481	1.2395	0.6602	0.3810	-1.7330	-1.6523	2.7936
GRA	0.6560	2.0697	1.2268	0.8265	0.4899	-1.6871	-1.4503	3.1059
MF	0.8421	2.5855	0.8286	0.5781	0.1853	-3.1203	-3.0696	2.7993
OSH	0.5161	0.8826	2.0621	0.2850	0.6658	-0.4280	-0.5581	1.3363
SAV	0.5270	1.3033	1.8952	0.3811	0.5542	-0.6877	-0.8600	1.7837
SNO	0.3090	1.4376	2.0744	0.3969	0.5727	-0.6930	-1.2075	2.0629
WAT	0.0236	1.9795	9.8240	0.4110	2.0399	-0.2015	-0.3652	2.2719
WET	0.7850	2.1410	1.1754	0.6828	0.3749	-1.8215	-2.0922	2.8770
WSA	0.6248	1.1538	1.5159	0.3468	0.4556	-0.7611	-1.2132	2.2010

A.2 Unseen Sites Test Set Performance by IGBP Category

Table 2: Test Set Performance by IGBP Category for Tower Sites Not Used in Training or Validation. The table probes the model's spatial transferability to new geographic locations.

IGBP	R^2	AU	AU Scaled	EU	EU Scaled	Pred	True	RMSE
CRO	0.4636	2.3466	0.9437	1.0999	0.4423	-2.4867	-1.9069	5.3958
DBF	0.6783	3.2219	0.7664	1.0417	0.2478	-4.2041	-4.2058	4.1673
ENF	0.659	2.4511	1.0033	0.7548	0.309	-2.443	-2.4021	3.3885
GRA	0.5507	1.4258	2.4560	0.4875	0.8397	-0.5805	-0.8304	2.8286
MF	0.804	3.0256	0.7730	0.7407	0.1893	-3.914	-3.7741	3.1610
OSH	0.3908	0.7437	2.3584	0.2436	0.7726	-0.3153	-0.2670	1.0284
WET	0.5904	1.6871	2.4805	0.5650	0.8306	-0.6802	-0.9129	2.4267